Ca^{2+} sensitivity of regulated cardiac thin filament sliding does not depend on myosin isoform

Brenda Schoffstall[1,2], Nicolas M. Brunet[1,2], Shanedah Williams[2], Victor F. Miller[2], Alyson T. Barnes[2], Fang Wang[2], Lisa A. Compton[2], Lori A. McFadden[2], Dianne W. Taylor[1,2], Margaret Seavy[2], Rani Dhanarajan[2] and P. Bryant Chase[1,2,3]

[1]*Institute of Molecular Biophysics,* [2]*Department of Biological Science and* [3]*Department of Chemical & Biomedical Engineering, Florida State University, Tallahassee, FL, USA*

Myosin heavy chain (MHC) isoforms in vertebrate striated muscles are distinguished functionally by differences in chemomechanical kinetics. These kinetic differences may influence the cross-bridge-dependent co-operativity of thin filament Ca^{2+} activation. To determine whether Ca^{2+} sensitivity of unloaded thin filament sliding depends upon MHC isoform kinetics, we performed *in vitro* motility assays with rabbit skeletal heavy meromyosin (rsHMM) or porcine cardiac myosin (pcMyosin). Regulated thin filaments were reconstituted with recombinant human cardiac troponin (rhcTn) and α-tropomyosin (rhcTm) expressed in *Escherichia coli*. All three subunits of rhcTn were coexpressed as a functional complex using a novel construct with a glutathione S-transferase (GST) affinity tag at the N-terminus of human cardiac troponin T (hcTnT) and an intervening tobacco etch virus (TEV) protease site that allows purification of rhcTn without denaturation, and removal of the GST tag without proteolysis of rhcTn subunits. Use of this highly purified rhcTn in our motility studies resulted in a clear definition of the regulated motility profile for both fast and slow MHC isoforms. Maximum sliding speed (pCa 5) of regulated thin filaments was roughly fivefold faster with rsHMM compared with pcMyosin, although speed was increased by 1.6- to 1.9-fold for regulated over unregulated actin with both MHC isoforms. The Ca^{2+} sensitivity of regulated thin filament sliding speed was unaffected by MHC isoform. Our motility results suggest that the cellular changes in isoform expression that result in regulation of myosin kinetics can occur independently of changes that influence thin filament Ca^{2+} sensitivity.

(Resubmitted 28 August 2006; accepted after revision 28 September 2006; first published online 5 October 2006)
Corresponding author P. B. Chase: Florida State University, Department of Biological Science, Bio Unit One, Tallahassee, FL 32306-4370, USA. Email: chase@bio.fsu.edu

Contraction of vertebrate striated muscle results from cyclic interactions between myosin in thick filaments and actin in thin filaments, with hydrolysis of MgATP as the chemical energy source. Actomyosin cross-bridge cycling is controlled by Ca^{2+}, and thin filament Ca^{2+} regulation may in turn be co-operatively influenced by cross-bridges (Gordon *et al.* 2000). Under physiological conditions, cross-bridge kinetics are determined by the specific type of myosin heavy chain (MHC) isoform(s) present in the muscle (Schiaffino & Reggiani, 1996). Less clearly defined, however, are the effects of MHC isoforms on Ca^{2+} control of myofilament function, particularly because multiple isoforms are normally present in the heart, and changes in MHC composition occur in cardiac disease.

Two MHC isoforms, α-MHC (fast) and β-MHC (slow), are expressed in mammalian cardiac muscle; β-MHC is also expressed in slow skeletal muscles while additional, faster isoforms are expressed in other skeletal muscles (Schiaffino & Reggiani, 1996). Muscle specific MHC isoform expression is variable among species. Ventricular myocardium is comprised of ∼97% β-MHC and ∼3% α-MHC in normal adult humans (Miyata *et al.* 2000), and is ∼70% β-MHC in adult rabbits (VanBuren *et al.* 1995). Rat ventricular myocardium transitions from predominately β-MHC in fetal and neonatal development to predominately (> 90%) α-MHC in young adults (Nakao *et al.* 1997).

Numerous investigations have compared ATP hydrolysis activity, isometric and single molecule force, cross-bridge cycling kinetics, and/or actin filament sliding speed between the fast α- *versus* slow β-MHC cardiac

B. Schoffstall and N. M. Brunet contributed equally to this work.

 DOI: 10.1113/jphysiol.2006.120105

isoforms (VanBuren *et al.* 1995; Palmiter *et al.* 1999; Krenz *et al.* 2003; Rundell *et al.* 2005). Isometric force generated by both isoforms is similar (Hasenfuss *et al.* 1991; Gibson *et al.* 1992; Metzger *et al.* 1999), while kinetic parameters that affect cardiac dynamics are significantly different (Palmiter *et al.* 1999). α-Myosin heavy chain has twice the actin-activated solution ATPase activity of β-MHC, and roughly three times the actin sliding speed (VanBuren *et al.* 1995). The latter is consistent with MgADP dissociation kinetics being roughly twofold faster for α-MHC (Palmiter *et al.* 1999). The rate of tension redevelopment (k_{TR}) decreases as expression of α-MHC decreases and β-MHC increases, and actomyosin cross-bridge cycling under high strain is 2.5- to threefold higher with α-MHC (Regnier *et al.* 2000; Rundell *et al.* 2005).

Calcium sensitivity has been compared between preparations containing α- and β-MHC cardiac isoforms under isometric (Pagani *et al.* 1986; Gibson *et al.* 1992; Metzger *et al.* 1999; Noguchi *et al.* 2003) and unloaded conditions (Noguchi *et al.* 2003). For these studies, rat or rabbit animal models were treated with propylthiouracil to induce hypothyroidism, levothyroxine to induce hyperthyroidism, or pressure overload to induce cardiac hypertrophy and failure. Abnormal thyroid states lead to expression of primarily α-MHC in hyperthyroidism and β-MHC in hypothyroidism or pressure overload, which are associated with altered contractile performance. In experimental designs where endogenous cardiac thin filament troponin (Tn) and tropomyosin (Tm) were included in the functional assays (Pagani *et al.* 1986; Gibson *et al.* 1992; Metzger *et al.* 1999), it is unknown whether the thin filament proteins were affected along with MHC composition as a result of thyroid conditioning or pressure overload.

Increased Ca^{2+} sensitivity of force has been reported for regulated preparations containing β-MHC compared with α-MHC (Gibson *et al.* 1992), while others reported no difference (Pagani *et al.* 1986). More recently, Metzger *et al.* (1999) found a rightward shift of the pCa–force relation with β-MHC, implying decreased Ca^{2+} sensitivity, while Noguchi *et al.* (2003) found a slight but not significant increase with α-MHC. These discrepancies have not been resolved and could be explained by Ca^{2+} sensitivity changes independent of myosin isoform shifts in response to imposed abnormal thyroid conditions and/or volume overload; they may instead result from shifts in thin filament or possibly other protein isoforms.

Clemmens *et al.* (2005) demonstrated the importance of Tn and Tm isoform matching for regulated thin filament function *in vitro* by varying regulatory protein isoform while myosin isoform was constant. For example, the Ca^{2+} dependence of thin filament sliding depended on whether cardiac or skeletal Tm was reconstituted with cardiac Tn (cTn). If abnormal thyroid conditions and/or pressure overload result in isoform changes in thin filament proteins *in vivo*, Ca^{2+} sensitivity could be altered. Thus, changes in Ca^{2+} sensitivity that were previously attributed to MHC isoform composition could instead result from changes in the thin filament. A thorough investigation of possible effects of fast *versus* slow MHC isoforms on Ca^{2+} sensitivity should include recombinant thin filament proteins that are not altered by any chemical or mechanical interventions. Noguchi *et al.* (2003) used extracted bovine Tn and Tm in their *in vitro* motility assays with thyroid condition-induced α-MHC and β-MHC, and found no change in pCa_{50}. The maximum speed in their experiments, however, differed by only ~1.5-fold. It is of interest to know whether representatives of extreme fast and slow MHC isoforms that have not been artificially induced affect Ca^{2+} sensitivity of thin filament sliding speed differently.

To determine whether the Ca^{2+} sensitivity of thin filament sliding depends upon MHC isoform, we compared *in vitro* motility assays using either rabbit skeletal heavy meromyosin (rsHMM) or porcine cardiac myosin (pcMyosin). Porcine cardiac myosin was used as the representative slow myosin isoform because it is very similar in composition (Chikuni *et al.* 2002) and kinetic behaviour (Malmqvist *et al.* 2004) to human cardiac myosin. Myosins extracted from normal pig or rabbit muscles provide models that have not been artificially altered by induction of a disease state. Regulated thin filaments were reconstituted with recombinant human α-Tm (rhcTm) and novel, coexpressed, recombinant human cardiac troponin (rhcTn). A GST tag on rhcTn allows more efficient purification compared with coexpressed but tagless rhcTn (Lohmann *et al.* 2001) and chicken skeletal Tn (Malnic & Reinach, 1994). Coexpression of all three subunits of rhcTn resulted in a highly functional protein with an apparent high affinity and specificity for actin–rhcTm and served as a constant regulator, unaffected by either disease state or endogenous muscle type. Thus we could rule out the possibility that thyroid disease states or pressure overload conditions contributed to our results. Our findings support the conclusions that differences between α-MHC and β-MHC may be exclusively kinetic (Palmiter *et al.* 1999), and that Tm and Tn isoforms are the major determinants of Ca^{2+} sensitivity (Clemmens *et al.* 2005) in cardiac muscle contraction.

Methods

Coexpression of recombinant human cardiac troponin

The genes for human cardiac troponin T (hcTnT; P45379-6), human cardiac troponin I (hcTnI; P19429) and human cardiac troponin C (hcTnC; P63316, AF020769) were cloned from a human heart cDNA library (BD Biosciences Clontech, Palo Alto, CA, USA)

and individually ligated into the pET 11d vector (Novagen-EMD Biosciences, San Diego, CA, USA). Human cardiac troponin T was moved into the pET 41a+ vector (Novagen-EMD Biosciences) at the *Nco*I and *Bam*HI restriction sites to create GST-rhcTnT with the GST tag at the N-terminus and a tobacco etch virus (TEV) protease cleavage site between GST and hcTnT. Human cardiac troponin I (*Stu*I and *Hin*d III restriction sites) and hcTnC (*Not*I and *Xho*I restriction sites), along with promoters and terminators, were sequentially moved into the same pET 41a+ vector. The final construct contained the genes for all three hcTn subunits (Fig. 1*A*). The sequence of each subunit was in agreement with the listed Swiss-Prot accession numbers except for hcTnI, D108G, which is located near the middle of the IT coiled-coil region (Takeda *et al.* 2003; Vinogradova *et al.* 2005).

To obtain functional troponin complex protein for this study, the above pET 41a+ hcTn expression plasmid containing all three subunits was transformed into BL21 STAR ultra-competent *Escherichia coli* cells (Invitrogen Corp., Carlsbad, CA, USA). Cultures were grown in 3 l of Luria broth (Sigma-Aldrich Co. St Louis, MO, USA) at 37°C until the optical density at 600 nm was 0.35–0.50, at which time protein expression was induced by addition of 0.4 mM Isopropyl B-D-1-thiogalactopyranoside (IPTG). Four hours after induction, cells were harvested, pelleted by centrifugation, and frozen at −80°C. Bacterial cell pellets were resuspended in GST Bind/Wash buffer (mM: 4.3 Na_2HPO_4, 1.47 KH_2PO_4, 137 NaCl and 2.7 KCl, pH 7.3) plus 2.5% streptomycin sulphate (Sigma), then subjected to two rounds of rapid freeze–thaw. An additional 2.5% streptomycin sulphate was added to precipitate nucleic acids. The sample was centrifuged, and the soluble crude bacterial lysate supernatant was dialysed overnight against GST Bind/Wash buffer at 4°C.

GST-rhcTn was purified by affinity chromatography (BioLogic LP Chromatography System, Bio-Rad, Hercules, CA, USA) using GST-Bind Resin (Novagen-EMD Biosciences, San Diego, CA, USA). GST-rhcTn was eluted with GST elution buffer (mM: 50 Tris-HCl, pH 9.5, and 10 reduced glutathione). Fractions containing protein (absorbance monitored continuously at A280 nM) were pooled, and concentration was determined using the Warburg-Christian method (DU 640 Spectrophotometer, Beckman Fullerton, CA, USA). The GST tag was cleaved from rhcTn by digestion with 50 i.u. AcTEV protease (Invitrogen) per milligram of fusion protein for 1.5 h at room temperature. Cleaved sample was dialysed overnight at 4°C against Tn dialysis and storage buffer (D&S buffer; mM: 125 imidazole-HCl, 125 KCl, 4 $MgCl_2$ and 2 $CaCl_2$ pH 7.0). The TEV protease cleavage site was introduced for removal of the affinity tag because we found in preliminary studies that several other commonly used proteases promiscuously cleaved rhcTnT (data not shown). After removal of the GST tag, the N-terminus of rhcTnT was extended by only one additional amino acid, a glycine.

The GST tag and TEV protease were separated from rhcTn by anion exchange chromatography (DE52 resin, Whatman, Maidstone, UK). GST tag and TEV protease eluted in the void volume by washing the loaded column with D&S buffer (Fig. 1*B*). Purified rhcTn eluted as a single

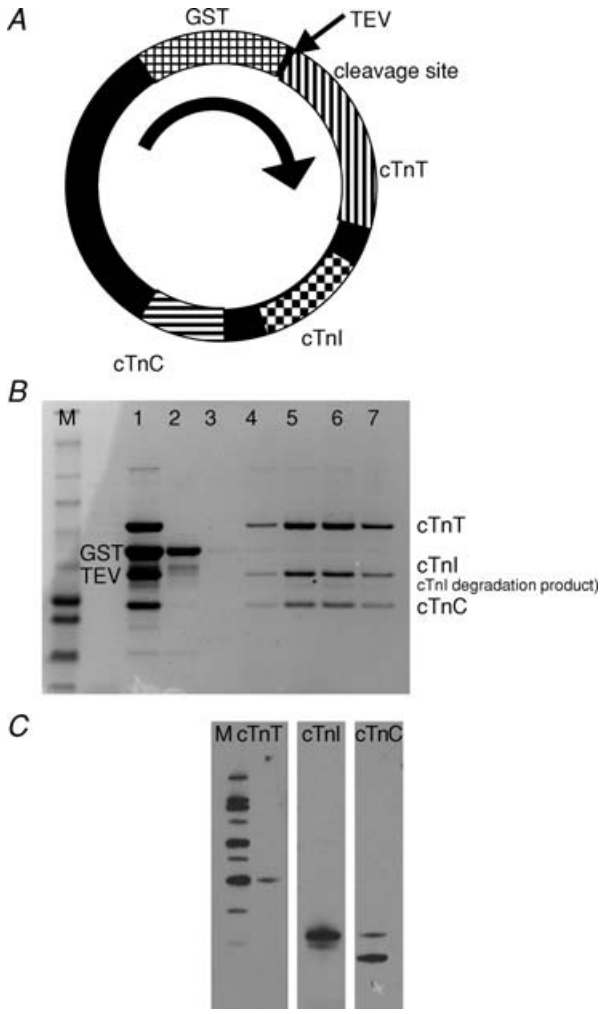

Figure 1. Coexpression of recombinant human cardiac troponin (rhcTn) complex
A, cDNA sequences for all three subunits of hcTn were cloned into pET 41a+ along with promotors and terminators for coexpression in *E. coli*. The plasmid was engineered with a GST tag at the N-terminus of hcTnT, and modified to include a TEV protease site between GST and hcTnT. *B*, SDS-PAGE analysis of the coexpressed rhcTn complex demonstrates that the three subunits form a complex; densitometry analysis indicates ∼96% purity. M, marker; 1, rhcTn complex after GST affinity purification and TEV protease cleavage; 2, anion exchange chromatography (DE52) void volume, containing GST tag and TEV protease; and 3–7, anion exchange chromatography fractions eluted by salt gradient. *C*, Western blot analysis of the coexpressed rhcTn complex. Specific antibodies for hcTnT (left), hcTnI (centre), and hcTnC (right) detected bands of the appropriate sizes for each subunit (see Methods). M, marker (MagicMark XP Western Protein Standard; Invitrogen).

peak by applying a salt gradient of 125 mM KCl to 400 mM. Fractions were analysed by SDS-PAGE (Fig. 1*B*), and pure rhcTn fractions were pooled. Typical yield from 3 l of culture was ∼0.7 mg purified rhcTn. Aliquots were stored at −80°C and used for motility assays within 2 weeks.

Coomassie-stained SDS-PAGE protein gels were imaged using an EDAS-290 digital imaging system (Kodak, Rochester, NY, USA), and band intensities were analysed with ImageJ 1.34s (National Institutes of Health, USA). Purity of rhcTn was ∼96% (Fig. 1*B*); we detected a small amount of rhcTnI degradation (Fig. 1*B* and *C*). Subunit stoichiometry was: rhcTnT, 0.99; rhcTnI, 0.90; and rhcTnC, 1.19 (expressed as percentage intensity rhcTn divided by the percentage intensity purified human cardiac Tn complex obtained from Research Diagnostics, Flanders, NJ, USA). Identity of the three subunits of rhcTn was confirmed by Western blot analysis (Fig. 1*C*) performed using the primary antibodies mouse anticardiac TnT, clone 1F11, mouse anticardiac TnC, clone 7B9, and mouse anticardiac TnI, clone 16A11 (Research Diagnostics, Flanders, NJ, USA) with the secondary antibody being goat antimouse HRP conjugate (Bio-Rad).

N-terminal sequencing and mass spectrometry of rhcTn

In preparation for Edman sequencing and mass spectrometry, rhcTn subunits were purified by reversed phase (RP) high-performance liquid chromatography (HPLC). A Beckman System Gold high-performance liquid chromatograph (Beckman-Coulter, Fullerton, CA, USA) equipped with a model 168 diode array detector, a model 126 solvent delivery system and a Rheodyne 7125 sample injection valve was used for RP chromatography. The rhcTn complex (50 μl of 0.26 μg μl^{-1}) was run on a Vydac C4 RP column (2.1 mm × 250 mm, The Nest Group, Southborough, MA, USA) using the standard solvent system of A = 0.1% trifluoroacetic acid (TFA) in water and B = 0.075% TFA in acetonitrile. Column effluent was monitored continuously at 220 and 280 nm, and fractions containing the predominant peaks were collected manually and concentrated by vacuum centrifugation.

N-Terminal sequencing was performed to verify the amino acid sequence of all three rhcTn subunits. Approximately 20% of each RP-HPLC purified peak was loaded onto a biobrene-treated glass fibre filter and subjected to 15 cycles of Edman degradation on a Procise 492 cLC (Applied Biosystems, Foster City, CA, USA) using standard methods. Analysis of each sequence identified the first RP peak as hcTnT, the second as hcTnI, and the third as hcTnC.

Matrix-assisted laser desorption/ionization time-of-flight (MALDI/TOF) mass spectrometry (MS) was performed on a Bruker Biflex III mass spectrometer (Bruker Daltonics, Billerica, MA, USA) equipped with a nitrogen laser (337 nm). Bruker software programs XACQ and XMASS were used for instrument control, data acquisition and data analysis. Reversed phase HPLC-purified rhcTnT, rhcTnI and rhcTnC fractions were diluted 1:5 in sinapinic acid (10 mg ml^{-1} in 50% acetonitrile, 0.1% TFA; Sigma) and 1 μl of each spotted onto the MALDI target. Approximately 200 laser shots were accumulated per sample.

Expression and purification of recombinant human α-tropomyosin

Human α-Tm was cloned by Dr F. Wang and expressed in *E. coli* as a fusion protein with maltose binding protein (MBP). Subsequently, the MBP tag was removed with thrombin before purifying the liberated recombinant α-Tm by HPLC using a Mono Q column (Pharmacia Biotech, Uppsala, Sweden). After removal of the MBP tag, recombinant Tm has two extra amino acids (GS-) at the N-terminus; GS- represents a conservative alternative to the AS- dipeptide in bacterially expressed Tm that substitutes functionally for N-terminal acetylation (Heald & Hitchcock-DeGregori, 1988; Monteiro *et al.* 1994).

Preparation of rabbit skeletal actin, rabbit skeletal myosin and porcine cardiac myosin

Florida State University's Institutional Animal Care and Use Committee approved all procedures and protocols involving vertebrate animals. Adult male New Zealand White rabbits were handled in accordance with the current National Institutes of Health/National Research Council *Guide for the Care and Use of Laboratory Animals.* Briefly, rabbits were injected I.M. with 3 mg acepromazine, 10 mg kg^{-1} xylazine and 50 mg kg^{-1} ketamine. Following verification of appropriate surgical depth of anaesthesia, the rabbits were exsanguinated via laceration of the carotid artery. The animals were then skinned, eviscerated and chilled on ice. Back and leg muscles were removed for acetone powder, or back muscles only for myosin preparation (Gordon *et al.* 1997; Chase *et al.* 2000; Schoffstall *et al.* 2005).

Actin was extracted from acetone powder prepared from rabbit back and leg muscles (Pardee & Spudich, 1982). Actin used for electron microscopic imaging was further purified on a Sepharose 6B-Cl column (GE Healthcare Bio-Sciences, Piscataway, NJ, USA). Rabbit skeletal myosin was prepared as previously described (Margossian & Lowey, 1982) and was subjected to mild chymotryptic digestion to obtain rabbit skeletal heavy meromyosin (rsHMM) (Kron *et al.* 1991). Porcine hearts were obtained from a local abattoir within 20 min of the animal's death. Porcine cardiac myosin (pcMyosin) was obtained from ventricular tissue as previously described (Schoffstall *et al.* 2006). ATP-insensitive 'dead heads' were

removed from rsHMM and pcMyosin preparations by ultracentrifugation in the presence of MgATP and F-actin on the day of use (Kron *et al.* 1991; Schoffstall *et al.* 2006).

Electron microscopy

Electron micrograph images of samples negatively stained with 2% uranyl acetate were recorded at ×45 000 magnification on a Philips CM120 electron microscope. Thin filaments were reconstituted by combining 0.45 μM G-actin and 0.02 μM rhcTm with or without 0.05–1.0 μM rhcTn in a solution comprising (mM): 10 imidazole, 2 Na_2PO_4, 50 KCl, 1 $MgCl_2$, 0.5 ATP, 0.5 DTT, and either 1 EGTA or 1 $CaCl_2$, pH 7.1 at 4°C. These were immediately used to produce lipid monolayer specimens as previously described for unregulated F-actin combined with α-actinin (Taylor *et al.* 2000). Actin–rhcTm or regulated thin filaments formed 2-D arrays on the monolayer within 2 h that appear to be stable for at least 3 months.

In vitro motility assays

In vitro motility assays were performed to measure the sliding speed of fluorescently labelled F-actin propelled by rsHMM or pcMyosin. Experimental protocols, solution preparation, flow cell preparation and analysis were essentially as previously described (Chase *et al.* 2000; Mihajlović *et al.* 2004). Assays were carried out at 30°C, with temperature in the flow cell maintained by circulating temperature-controlled water through a copper coil around the objective. F-actin was fluorescently labelled with rhodamine phalloidin (RhPh). Immediately before the motility assay, equimolar concentrations of rhcTn and rhcTm were applied to the labelled F-actin in the flow cell with a 'wash' of actin buffer (AB), composed of (mM): 25 KCl, 25 imidazole titrated to pH 7.4 with HCl, 4 $MgCl_2$, 1 EGTA and 1 DTT. Solution composition for assays with regulated RhPh-labelled F-actin was calculated as described previously (Köhler *et al.* 2003; Liang *et al.* 2003). Solutions contained (mM): 2 MgATP, 1 Mg^{2+}, 10 EGTA, sufficient $Ca(CH_3COO)_2$ to achieve the desired pCa (pCa 9–4), 50 K^+, 15 Na^+, 20 Mops, pH 7.00 at 30°C, 0.3% methyl cellulose (MC), and rhcTn and rhcTm. Ionic strength was adjusted to 0.085 M with TrisOH and acetic acid. To minimize photobleaching of the fluorophores and photo-oxidative damage to the proteins, 3 mg ml^{-1} glucose, 100 μg ml^{-1} glucose oxidase, 18 μg ml^{-1} catalase and 40 mM DTT were added to motility buffers.

Fluorescence microscopy, data acquisition and analysis

Rhodamine phalloidin-labelled F-actin motility was observed by fluorescence microscopy on a Reichart Diastar microscope at ×100 magnification with Hg lamp illumination, imaging six to eight fields from varying areas on the flow cell, as previously described (Schoffstall *et al.* 2005). Field images were recorded as 30 s clips using a VE1000 SIT camera (Dage-MTI, Inc., Michigan City, IN, USA) and a Panasonic AG-7350 videocassette recorder. Analysis of motility speed was carried out with the aid of MetaMorph software, Molecular Devices Corp, Downingtown, PA, USA as previously described (Mihajlović *et al.* 2004). Stacks of 90–150 frames for each experiment were created from digitized movies; actin filament paths were visualized by superimposing all frames of one stack to form a projection and subtracting the image of the last frame (Fig. 2). For each stack, four to eight filaments were randomly selected, and the distance travelled (d) was estimated by manually measuring the contour lines of their respective pathways (Fig. 2*B*). Speed was determined as $d/\Delta t$(no. of frames − 1), where Δt ($\Delta t = 0.0333$ s) is determined by the 30 frames per second (f.p.s.) video recording.

Non-linear regression analysis was performed using SigmaPlot software (version 8.0; SPSS, Inc., Port

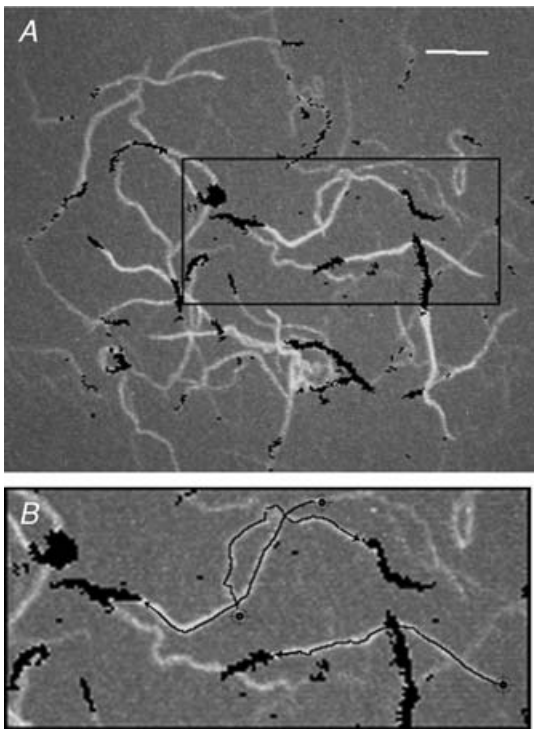

Figure 2. Analysis of actin motility
A, superposition of 90 sequential video frames from one representative recorded fluorescence microscopy field. White traces indicate the paths of RhPh-labelled actin filaments over 3 s. Actin filaments in the last frame are indicated in black. Scale bar 10 μm. *B*, rectangular area from *A* magnified to illustrate measurement of the distance travelled by the trailing ends of three actin filaments. The trailing end of each actin filament is marked with a dot in the first frame and with an arrowhead in the 90th frame. Each path contour begins at the dot and proceeds to the arrowhead. Hence, the arrowheads also represent the direction of filament sliding.

Richmond, CA, USA) to fit pCa dependence of filament sliding speed (s), weighted by the fraction of filaments moving uniformly, to the Hill equation:

$$s = \frac{s_{\max}}{(1 + 10^{n_H(pCa - pCa_{50})})} \quad (1)$$

where regression parameter s_{max} represents the maximal value obtained at high [Ca^{2+}] (low pCa), pCa_{50} is equal to the pCa at the mid-point of the relationship (i.e. for s = $s_{max}/2$), and n_H describes the steepness of the relationship around pCa_{50}. Where expressed, regression errors are standard errors for the regression parameters.

Results

Characterization of the coexpressed recombinant human cardiac troponin complex

To obtain rhcTn that has consistent subunit composition and is unaffected by post-translational modifications in mammalian cells, we developed a construct for coexpression of rhcTn in *E. coli* (see Methods). Highly purified, functional rhcTn complex was obtained from bacterial lysate via two chromatography steps (see Methods, Fig. 1), eliminating the need for denaturation and renaturation. N-Terminal sequencing and mass spectrometry of our coexpressed rhcTn complex are consistent with expected results for three subunits: rhcTnT, rhcTnI and rhcTnC. N-Terminal sequencing indicated that there was an extra glycine at the N-terminus of rhcTnI preceding the normal methionine start. Sequencing of rhcTnC yielded two populations, one with an N-terminal glycine and the other with a methionine–glycine preceding the normal methionine start. These one or two amino acid extensions of rhcTnI and rhcTnC were introduced with 5′ restriction enzyme sites during plasmid design. As expected with the TEV protease cleavage site, rhcTnT included one extra glycine at the N-terminus preceding the normal methionine start.

The protonated molecular weights measured by mass spectrometry were 34 629 Da for rhcTnT (calculated value 34 647 Da), 23 992 Da for rhcTnI (calculated value 24 006 Da) and 18 334 Da for rhcTnC (calculated value 18 330 Da), and were within the expected range for the methodology used. Gel densitometry analysis confirmed that the subunits of the complex were expressed and purified in a 1:1:1 ratio (see Methods). Transmission electron microscopic (TEM) images of negatively stained, reconstituted thin filaments on a positively charged lipid surface (see Methods) reveal periodically spaced (~38 nm) densities (Fig. 3*B*) not observed on actin–rhcTm (Fig. 3*A*). This spacing is consistent with physiological binding of rhcTn to actin–rhcTm. This highly purified rhcTn protein was used as a control regulator to compare thin filament sliding speed over slow and fast MHC isoforms in the *in vitro* motility assay.

Establishment of the optimal concentration of regulatory proteins for *in vitro* motility assays

Recombinant hcTn and rhcTm were added in the physiological 1:1 stoichiometric ratio for reconstitution of thin filaments in regulated motility assays. We first determined the concentration of rhcTn (and rhcTm) necessary to regulate motility for both rsHMM and pcMyosin in the *in vitro* motility assay by titration of regulatory protein concentrations (Fig. 4). We found that 15 nM of rhcTn (and 15 nM rhcTm) was both necessary and sufficient to inhibit motility at pCa 9 and to achieve maximum speed at pCa 5 for both rsHMM and pcMyosin (Fig. 4). The maximum sliding speeds for both MHC isoforms were 1.6- to 1.9-fold faster than those obtained with unregulated F-actin. Because this regulatory protein concentration (15 nM) is lower than that typically necessary for regulated *in vitro* motility studies utilizing reconstituted, individually expressed subunits of recombinant Tn (Burkart *et al.* 2003; Köhler *et al.* 2003), we conclude that our coexpressed rhcTn complex has a higher apparent affinity for actin–Tm than reconstituted recombinant Tn complexes. This may be attributed to proper folding and efficient quaternary structure formation that is only achievable in the cellular environment. Furthermore, TEM images provide strong evidence for physiologically relevant binding of coexpressed rhcTn to actin–rhcTm (Fig. 3).

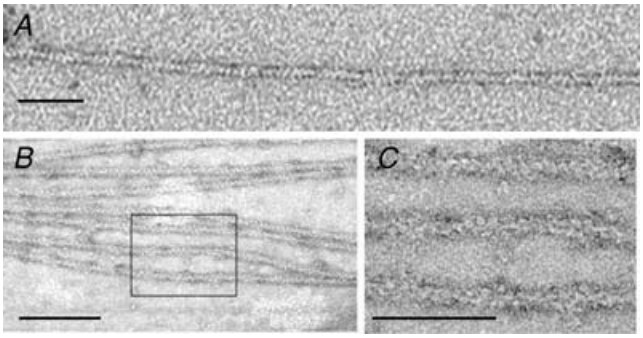

Figure 3. Transmission electron micrographs of negatively stained F-actin–rhcTm–EGTA (*A*) and F-actin–rhcTm–rhcTn–EGTA complexes on positively charged lipid monolayers (*B* and *C*)
C is the rectangular area in *B*, magnified. The scale bars represent 50 nm in *A*, 100 nm in *B* and 50 nm in *C*. Areas of additional density on the regulated thin filaments in *B* and *C* indicate physiological binding of the rhcTn complex to actin–rhcTm.

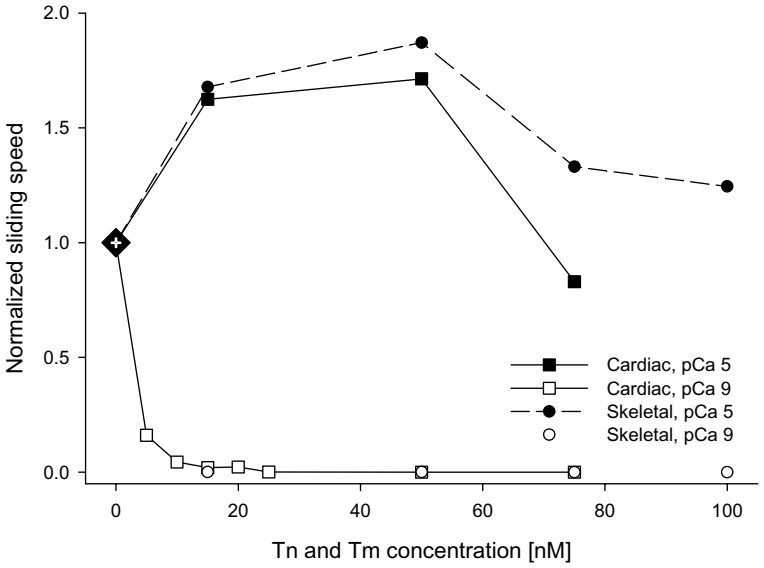

Figure 4. Effect of recombinant human cardiac regulatory protein concentration on motility at pCa 9 (open symbols) and pCa 5 (filled symbols)
Thin filaments were reconstituted with equimolar concentrations of rhcTn and rhcTm added to flow cells (see Methods). Assays were conducted using pcMyosin (squares) or rsHMM (circles). Speeds were normalized to unregulated motility for each myosin isoform (large diamond at 0 nM rhcTn and rhcTm). Note that at concentrations $\geq$ 15 nM, regulatory proteins fully inhibited filament sliding at pCa 9. Also note that over the range of 15–50 nM rhcTn and rhcTm, regulated thin filament sliding speed was substantially faster than for unregulated actin.

Effects of MHC isoform on regulated thin filament sliding

Motility assays were used to investigate the Ca^{2+} sensitivity of regulated thin filament sliding without the effects of internal loads that are present in fibre bundles or myocyte preparations. By utilizing our purified rhcTn complex and rhcTm, the regulatory proteins were constant in all experiments, while MHC isoform and [Ca^{2+}] were varied. Additionally, we used extracted myosin from normal animal models; no artificial intervention was used to obtain the fast skeletal and slow cardiac β-MHC isoforms. The value of s_{max} (eqn (1)) was $7.1 \pm 0.6\ \mu m\ s^{-1}$ with rsHMM and $1.4 \pm 0.1\ \mu m\ s^{-1}$ with pcMyosin β-MHC. This fivefold difference was expected owing to the slower kinetics and increased attachment time of the slow β-MHC isoform relative to that of fast skeletal myosin and is larger than the difference between cardiac isoforms from a single species (Metzger *et al.* 1999; Palmiter *et al.* 1999; Köhler *et al.* 2003; Noguchi *et al.* 2003; Rundell *et al.* 2005).

The discrepancy that we sought to resolve was whether the Ca^{2+} sensitivity of thin filament sliding was affected by myosin isoform. Sliding speed was observed to be a sigmoidal function of pCa for both pcMyosin (Fig. 5*A*) and rsHMM (Fig. 5*B*). Surprisingly, our data revealed that pCa_{50} did not change with MHC isoform (Fig. 5): pCa_{50} was 5.77 ± 0.04 for rsHMM and 5.72 ± 0.02 for pcMyosin. Co-operativity parameter n_H was 4.7 ± 1.7 for rsHMM and 6.1 ± 1.9 for pcMyosin. These results suggest that, when the regulatory proteins are maintained as a constant, Ca^{2+} sensitivity of regulated thin filament function is unaffected by actomyosin kinetics.

To determine whether our results could possibly be attributed to the lower concentration of rhcTn (and rhcTm) used in the *in vitro* motility assay (compared to previously published work), we performed additional experiments with 50 nM rhcTn and rhcTm (data not shown). The value of pCa_{50} was 5.65 ± 0.03 for rsHMM and 5.60 ± 0.07 for pcMyosin. Co-operativity parameter n_H was 3.0 ± 0.5 for rsHMM and 2.0 ± 0.6 for pcMyosin. Although there were small differences in the results obtained at 15 *versus* 50 nM regulatory proteins, we found no difference in Ca^{2+} sensitivity between fast and slow MHC isoforms at either concentration.

Discussion

The major finding of this study was that the Ca^{2+} sensitivity of human cardiac thin filament sliding is not dependent upon the kinetics of active cross-bridge cycling when MHC isoform is varied. This suggests that any influence of cross-bridge-dependent activation of the cardiac thin filament is not affected by myosin kinetics during unloaded filament sliding. In addition, discrepant results from earlier investigations (Pagani *et al.* 1986; Gibson *et al.* 1992; Metzger *et al.* 1999) may have occurred owing to other factors that influence Ca^{2+} sensitivity and are concomitant with experimentally induced changes in MHC. Thus, physiological tuning of myosin kinetics and efficiency in the heart appear to be separable from changes in Ca^{2+} responsiveness of contractility.

Our experiments were facilitated by a novel GST tag coexpression and purification of the three subunits of recombinant human cardiac troponin. Using this protocol, we were efficiently able to obtain a highly purified recombinant hcTn complex (Fig. 1) that could be used with rhcTm as a Ca^{2+} regulator of thin filament sliding in the *in vitro* motility assay. Our coexpressed rhcTn is preferable to individually expressed and reconstituted Tn subunits primarily because of ease of purification. Although other coexpression methods for the three

Tn subunits have previously been presented (Malnic & Reinach, 1994; Lohmann *et al.* 2001), our purification strategy is more efficient, with GST affinity as the first of two simple purification steps (Fig. 1 and Methods). Our data indicate that folding of the protein complex as it is expressed in the cellular environment leads to a Tn complex that has an apparent high affinity for Tm–actin (Fig. 4), and that forms reconstituted thin filaments with native structure (Fig. 3). We designed our *in vitro* studies so that the MHC isoform could be altered independent of the Tn and Tm isoform. Rabbit skeletal (fast) HMM and porcine cardiac (slow) myosin exhibit a fivefold difference in maximum speed (Fig. 5), and thus reflect the wide range of variation of myosin kinetics within striated muscles of a given higher vertebrate.

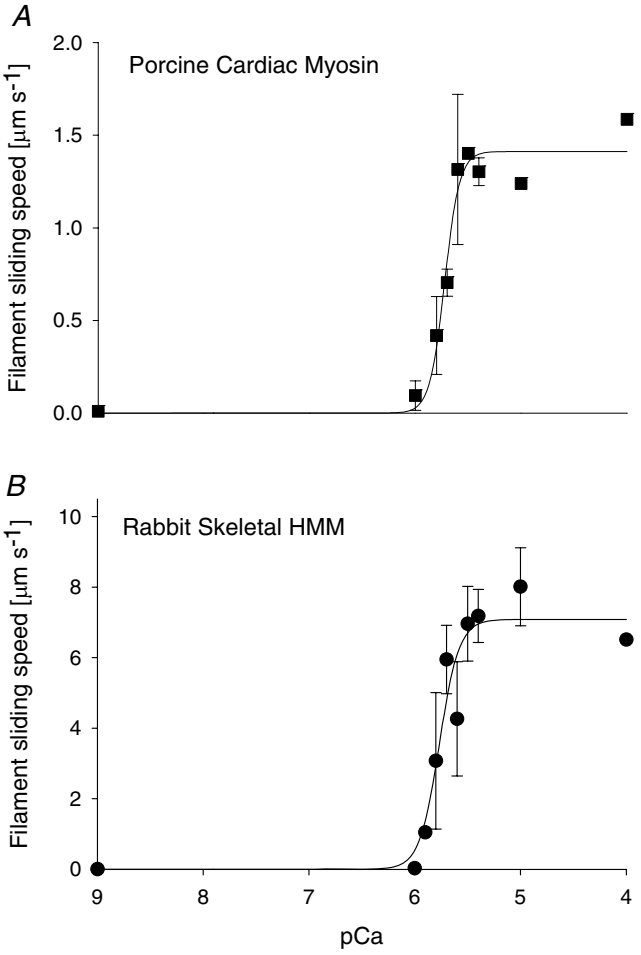

Figure 5. Ca^{2+} sensitivity of sliding speed for regulated thin filaments propelled by pcMyosin (β-MHC, *A*) or rsHMM (*B*)
Thin filaments were reconstituted with 15 nM rhcTn and 15 nM rhcTm. Each point represents the average thin filament sliding speed ($n = \sim$90 filaments for 2 flow cells) at the given pCa. Error bars represent standard deviation. The curves represent non-linear least squares regression fits to the Hill Equation (eqn (1)). There was no significant difference in the regression parameter estimates of pCa_{50} or n_H (eqn (1)) between pcMyosin and rsHMM (see Results).

Homogeneity of Tn and Tm isoform is important when examining Ca^{2+} sensitivity of cross-bridge cycling (Clemmens *et al.* 2005). In rat cardiac muscle, Ca^{2+}-mediated thin filament activation is limiting to the rate of isometric force development, regardless of MHC isoform (Regnier *et al.* 2004). These data, together with our data presented here (Fig. 5), suggest that Tn and Tm isoforms, rather than myosin cycling speed (which depends on myosin isoform), are the primary determinants of Ca^{2+} sensitivity of thin filament sliding *in vitro*. In previous Ca^{2+} sensitivity studies (Pagani *et al.* 1986; Gibson *et al.* 1992; Metzger *et al.* 1999; Noguchi *et al.* 2003), variations in MHC isoform were secondary to chemically induced thyroid state or physical aortic banding, which may have also altered the isoforms of Tn and Tm or other proteins that influence Ca^{2+} sensitivity *in vivo*. It is therefore possible that previously reported differences in pCa_{50} resulted from changes in protein isoforms other than myosin.

Given the kinetic differences between fast and slow MHC isoforms, the result shown in Fig. 5 is somewhat surprising, since slowly cycling myosin would be expected to have a larger effect on cross-bridge-dependent co-operative activation of the thin filament. The attached time for a fast myosin must be shorter than for a slow myosin, as evidenced by faster ATPase rates and actin sliding speeds for α-MHC than for β-MHC (Sugiura *et al.* 1998; Alpert *et al.* 2002). The fraction of the total actomyosin cross-bridge cycle for which myosin is attached to actin (the duty ratio) may be the same or different for fast *versus* slow MHC isoforms, depending on whether the attached time varies in proportion to the total cross-bridge cycle time. The duty ratio for β-MHC under loaded conditions appears to be greater than that for α-MHC in large mammals (rabbits and humans), while these duty ratios are similar in small rodents (rats and mice) (Alpert *et al.* 2002; Noguchi *et al.* 2003). By relating the duty cycle to the average force per cross-bridge and the constant unitary force, the duty ratio for fast skeletal and β-cardiac myosins (our models for this study) has been estimated to be approximately the same (Harris *et al.* 1994).

Since myocytes shorten during the cardiac cycle, it is of interest to understand how the extremes of fast or slow MHC isoforms may or may not affect Ca^{2+} sensitivity under both unloaded and isometric conditions. In this study, we focused on Ca^{2+} sensitivity during unloaded sliding for fast and slow MHC isoforms. The conclusions from this study might not necessarily apply to the isometric portion of the cardiac cycle, although factors that affect Ca^{2+} sensitivity in unloaded conditions most often affect isometric force in a similar manner. During unloaded filament sliding, duty ratio estimates typically range from $\sim$1 to 5% while, in contrast, estimates range from $\sim$20 to 40% (or higher) during isometric contraction, where the kinetics of ADP release and cross-bridge dissociation are

slower. We anticipate the same relative reduction in duty ratio for fast and slow myosin when comparing isometric with unloaded conditions. Cross-bridge-dependent effects on thin filament activation (Vibert *et al.* 1997) and co-operativity (N. Brunet, unpublished observations) can be detected not only under isometric, but also under unloaded conditions. We found no difference in the Ca^{2+} sensitivity between fast rsHMM and slow pcMyosin (Fig. 5). The estimate of duty ratio for rsHMM is ∼5% (Uyeda *et al.* 1990), but there is no previously determined estimate for pcMyosin. Our results would imply that the duty ratios are similar for the two myosins studied if duty ratio is an important determinant of Ca^{2+} sensitivity rather than cross-bridge cycling kinetics *per se*. It also follows that longer attachment time (pcMyosin) does not affect the Ca^{2+} sensitivity of thin filament sliding.

There are both practical and physiologically relevant implications of our findings. Skeletal myosin and HMM has historically been more widely used for *in vitro* motility studies than cardiac myosin because it is easier to obtain high quality preparations routinely and is more stable in storage. Additionally, the fast sliding speed makes differences and changes in speed easier to resolve during analysis. This investigation has validated the use of skeletal HMM for *in vitro* motility studies with cardiac thin filament proteins; the proportional increase in maximum sliding speed over unregulated speed is similar between both MHC isoforms tested, even though there is a difference in absolute speed (Figs 4 and 5). Additionally, pCa_{50} is the same for both fast skeletal HMM and slow cardiac myosin when tested with the same recombinant cardiac thin filament proteins (Fig. 5). We find that the cross-bridge cycle time does not influence the Ca^{2+} sensitivity of cardiac thin filament sliding. This has implications for cardiac function in cases where myosin isoforms transition from faster α-MHC to the slower β-MHC, as occurs during the progression of human heart failure (Miyata *et al.* 2000) and other disease processes, as well as during normal developmental processes (Schiaffino & Reggiani, 1996). Our data suggest that cellular regulation of myosin kinetics (particularly isoform expression) can occur independently of changes that may influence thin filament Ca^{2+} sensitivity.

References

Alpert NR, Brosseau C, Federico A, Krenz M, Robbins J & Warshaw DM (2002). Molecular mechanics of mouse cardiac myosin isoforms. *Am J Physiol Heart Circ Physiol* **283**, H1446–H1454.

Burkart EM, Sumandea MP, Kobayashi T, Nili M, Martin AF, Homsher E & Solaro RJ (2003). Phosphorylation or glutamic acid substitution at protein kinase C sites on cardiac troponin I differentially depress myofilament tension and shortening velocity. *J Biol Chem* **278**, 11265–11272.

Chase PB, Chen Y, Kulin KL & Daniel TL (2000). Viscosity and solute dependence of F-actin translocation by rabbit skeletal heavy meromyosin. *Am J Physiol Cell Physiol* **278**, C1088–C1098.

Chikuni K, Tanabe R, Muroya S & Nakajima I (2002). Comparative sequence analysis of four myosin heavy chain isoforms expressed in porcine skeletal muscles: sequencing and characterization of the porcine myosin heavy chain slow isoform. *Anim Sci J* **73**, 257–262.

Clemmens EW, Entezari M, Martyn DA & Regnier M (2005). Different effects of cardiac *versus* skeletal muscle regulatory proteins on *in vitro* measures of actin filament speed and force. *J Physiol* **566**, 737–746.

Gibson LM, Wendt IR & Stephenson DG (1992). Contractile activation properties of ventricular myocardium from hypothyroid, euthyroid and juvenile rats. *Pflugers Arch* **422**, 16–23.

Gordon AM, Homsher E & Regnier M (2000). Regulation of contraction in striated muscle. *Physiol Rev* **80**, 853–924.

Gordon AM, LaMadrid MA, Chen Y, Luo Z & Chase PB (1997). Calcium regulation of skeletal muscle thin filament motility in vitro. *Biophys J* **72**, 1295–1307.

Harris DE, Work SS, Wright RK, Alpert NR & Warshaw DM (1994). Smooth, cardiac and skeletal muscle myosin force and motion generation assessed by cross-bridge mechanical interactions in vitro. *J Muscle Res Cell Motil* **15**, 11–19.

Hasenfuss G, Mulieri LA, Blanchard EM, Holubarsch C, Leavitt BJ, Ittleman F & Alpert NR (1991). Energetics of isometric force development in control and volume-overload human myocardium. Comparison with animal species. *Circ Res* **68**, 836–846.

Heald RW & Hitchcock-DeGregori SE (1988). The structure of the amino terminus of tropomyosin is critical for binding to actin in the absence and presence of troponin. *J Biol Chem* **263**, 5254–5259.

Köhler J, Chen Y, Brenner B, Gordon AM, Kraft T, Martyn DA, Regnier M, Rivera AJ, Wang CK & Chase PB (2003). Familial hypertrophic cardiomyopathy mutations in troponin I (K183Δ, G203S, K206Q) enhance filament sliding. *Physiol Genomics* **14**, 117–128.

Krenz M, Sanbe A, Bouyer-Dalloz F, Gulick J, Klevitsky R, Hewett TE, Osinska HE, Lorenz JN, Brosseau C, Federico A, Alpert NR, Warshaw DM, Perryman MB, Helmke SM & Robbins J (2003). Analysis of myosin heavy chain functionality in the heart. *J Biol Chem* **278**, 17466–17474.

Kron SJ, Toyoshima YY, Uyeda TQ & Spudich JA (1991). Assays for actin sliding movement over myosin-coated surfaces. *Meth Enzymol* **196**, 399–416.

Liang B, Chen Y, Wang CK, Luo Z, Regnier M, Gordon AM & Chase PB (2003). Ca^{2+} regulation of rabbit skeletal muscle thin filament sliding: role of cross-bridge number. *Biophys J* **85**, 1775–1786.

Lohmann K, Westerdorf B, Maytum R, Geeves MA & Jaquet K (2001). Overexpression of human cardiac troponin in *Escherichia coli*: its purification and characterization. *Protein Expr Purif* **21**, 49–59.

Malmqvist UP, Aronshtam A & Lowey S (2004). Cardiac myosin isoforms from different species have unique enzymatic and mechanical properties. *Biochemistry* **43**, 15058–15065.

Malnic B & Reinach FC (1994). Assembly of functional skeletal muscle troponin complex in *Escherichia coli*. *Eur J Biochem* **222**, 49–54.

Margossian SS & Lowey S (1982). Preparation of myosin and its subfragments from rabbit skeletal muscle. *Methods Enzymol* **85** Part B, 55–71.

Metzger JM, Wahr PA, Michele DE, Albayya F & Westfall MV (1999). Effects of myosin heavy chain isoform switching on Ca^{2+}-activated tension development in single adult cardiac myocytes. *Circ Res* **84**, 1310–1317.

Mihajlović G, Brunet NM, Trbović J, Xiong P, Molnár SV & Chase PB (2004). All-electrical switching and control mechanism for actomyosin-powered nanoactuators. *Appl Phys Lett* **85**, 1060–1062.

Miyata S, Minobe W, Bristow MR & Leinwand LA (2000). Myosin heavy chain isoform expression in the failing and nonfailing human heart. *Circ Res* **86**, 386–390.

Monteiro PB, Lataro RC, Ferro JA & Reinach FdeC (1994). Functional α-tropomyosin produced in *Escherichia coli.* A dipeptide extension can substitute the amino-terminal acetyl group. *J Biol Chem* **269**, 10461–10466.

Nakao K, Minobe W, Roden R, Bristow MR & Leinwand LA (1997). Myosin heavy chain gene expression in human heart failure. *J Clin Invest* **100**, 2362–2370.

Noguchi T, Camp P Jr, Alix SL, Gorga JA, Begin KJ, Leavitt BJ, Ittleman FP, Alpert NR, LeWinter MM & VanBuren P (2003). Myosin from failing and non-failing human ventricles exhibit similar contractile properties. *J Mol Cell Cardiol* **35**, 91–97.

Pagani ED, Shemin R & Julian FJ (1986). Tension-pCa relations of saponin-skinned rabbit and human heart muscle. *J Mol Cell Cardiol* **18**, 55–66.

Palmiter KA, Tyska MJ, Dupuis DE, Alpert NR & Warshaw DM (1999). Kinetic differences at the single molecule level account for the functional diversity of rabbit cardiac myosin isoforms. *J Physiol* **519**, 669–678.

Pardee JD & Spudich JA (1982). Purification of muscle actin. *Methods Enzymol* **85** Part B, 164–181.

Regnier M, Martin H, Barsotti RJ, Rivera AJ, Martyn DA & Clemmens E (2004). Cross-bridge versus thin filament contributions to the level and rate of force development in cardiac muscle. *Biophys J* **87**, 1815–1824.

Regnier M, Rivera AJ, Chen Y & Chase PB (2000). 2-Deoxy-ATP enhances contractility of rat cardiac muscle. *Circ Res* **86**, 1211–1217.

Rundell VL, Manaves V, Martin AF & De Tombe PP (2005). Impact of β-myosin heavy chain isoform expression on cross-bridge cycling kinetics. *Am J Physiol Heart Circ Physiol* **288**, H896–H903.

Schiaffino S & Reggiani C (1996). Molecular diversity of myofibrillar proteins: gene regulation and functional significance. *Physiol Rev* **76**, 371–423.

Schoffstall B, Clark AN & Chase PB (2006). Positive inotropic effects of low dATP/ATP ratios on mechanics and kinetics of porcine cardiac muscle. *Biophys J* **91**, 2216–2226.

Schoffstall B, Kataoka A, Clark A & Chase PB (2005). Effects of rapamycin on cardiac and skeletal muscle contraction and crossbridge cycling. *J Pharmacol Exp Ther* **312**, 12–18.

Sugiura S, Kobayakawa N, Fujita H, Yamashita H, Momomura S, Chaen S, Omata M & Sugi H (1998). Comparison of unitary displacements and forces between 2 cardiac myosin isoforms by the optical trap technique: molecular basis for cardiac adaptation. *Circ Res* **82**, 1029–1034.

Takeda S, Yamashita A, Maeda K & Maéda Y(2003). Structure of the core domain of human cardiac troponin in the Ca^{2+}-saturated form. *Nature* **424**, 35–41.

Taylor KA, Taylor DW & Schachat F (2000). Isoforms of α-actinin from cardiac, smooth, and skeletal muscle form polar arrays of actin filaments. *J Cell Biol* **149**, 635–646.

Uyeda TQ, Kron SJ & Spudich JA (1990). Myosin step size. Estimation from slow sliding movement of actin over low densities of heavy meromyosin. *J Mol Biol* **214**, 699–710.

VanBuren P, Harris DE, Alpert NR & Warshaw DM (1995). Cardiac V1 and V3 myosins differ in their hydrolytic and mechanical activities in vitro. *Circ Res* **77**, 439–444.

Vibert P, Craig R & Lehman W (1997). Steric-model for activation of muscle thin filaments. *J Mol Biol* **266**, 8–14.

Vinogradova MV, Stone DB, Malanina GG, Karatzaferi C, Cooke R, Mendelson RA & Fletterick RJ (2005). Ca^{2+}-regulated structural changes in troponin. *Proc Natl Acad Sci U S A* **102**, 5038–5043.

Acknowledgements

We would like to express our gratitude to Bradley's Country Store, Tallahassee, FL, USA for providing the porcine hearts and to Dr Gregg G. Hoffman for advice on protein purification. This work was supported by NIH/NHLBI HL63974 (P.B.C.), NIH/NIAMS AR47421 (Dr K. A. Taylor) and predoctoral fellowships from American Heart Association FL/PR Affiliate (N.M.B. and L.A.C.) and Florida State University's Center for Materials Research and Technology (MARTECH; B.S.).

Authors' present addresses

S. Williams: Taxolog, Inc., Tallahassee, FL, USA.

V. F. Miller and L. A. Compton: Fisher Scientific, Suwanee, GA, USA.

A. T. Barnes: University of the Pacific Dugoni School of Dentistry, San Francisco, CA, USA.

F. Wang: The Institute of Genetic Engineering, Southern Medical University, Guangzhou, P. R. China.